

Critical composition dependence of the hydrogenation of $\text{Mg}_{2\pm\delta}\text{Ni}$ thin films

D.M. Borsa^{a,*}, W. Lohstroh^b, R. Gremaud^a, J.H. Rector^a,
B. Dam^a, R.J. Wijngaarden^a, R. Griessen^a

^a Faculty of Sciences, Department of Physics and Astronomy, Condensed Matter Physics, Vrije Universiteit,
De Boelelaan 1081, 1081 HV Amsterdam, The Netherlands

^b Forschungszentrum Karlsruhe GmbH, Institut für Nanotechnologie, 76021 Karlsruhe, Germany

Received 7 February 2006; received in revised form 20 March 2006; accepted 21 March 2006

Available online 5 May 2006

Abstract

The hydrogenation of metallic Mg_2Ni films was shown to proceed via a self-organized double layering of transparent Mg_2NiH_4 and metallic $\text{Mg}_2\text{NiH}_{0.3}$. For stoichiometries departing from Mg_2Ni we conclude from optical reflection, transmission and electrical measurements that the hydrogenation process involves two competing effects: (i) the nucleation of the initial Mg_2NiH_4 layer near the substrate and the ensuing growth of this layer and (ii) the slow random nucleation of the same phase within the remaining part of the film. Which process dominates depends critically on the stoichiometry of the parent metal alloy.

© 2006 Elsevier B.V. All rights reserved.

Keywords: Light absorption and reflection; Hydrogen storage materials; Thin films

1. Introduction

In 2002 Isidorsson et al. [1] reported on a remarkable reflector-to-absorber transition in Mg_2NiH_y hydride films. This transition, which occurs at low overall hydrogen concentration was at that time rather intriguing since the measured physical properties (optical reflection, transmission and electrical resistivity) were not compatible with the assumption of a homogeneous sample. It took some time before Lohstroh et al. [2,7] succeeded in demonstrating that the strongly absorbing state was due to a self-organized two-layer (phase) nucleation and growth process. The complete hydrogenation of Mg_2Ni results in the formation of Mg_2NiH_4 . This phase is transparent with an optical band gap [2] of ~ 1.9 eV and contains 3.6 wt% of hydrogen [6]. Mg_2NiH_4 is an example of a complex hydride with potential both as a smart window and as a hydrogen storage material. During its reflector-to-absorber transition, the overall absorption in the solar range of Mg_2NiH_y changes from 40 to 84% while its thermal emissivity changes from 0.10 to 0.17

[3]. This combination of properties makes Mg–Ni hydrides interesting candidates as active layer in variable solar absorber devices [4,5]. Having such applications in view, understanding the details of the hydrogen uptake of this material is of crucial importance. In particular it is important to investigate the role of the parent metal composition on the hydrogenation process during the reflector-to-absorber transition. In the first stages of the hydrogenation process, the $\text{Mg}_{2\pm\delta}\text{NiH}_y$ films consist of a self-organized double layer structure: a transparent Mg_2NiH_4 layer at the substrate–film interface and a top layer of $\text{Mg}_2\text{NiH}_{0.3}$. This so-called black state does not depend on composition. In this article we show that the nature of the ensuing hydrogenation process depends critically on the composition of the parent metal alloy. While hydrogenation of Mg_yNi films with $2 < y < 2.5$ proceeds by a random nucleation and growth of the Mg_2NiH_4 phase within the metallic top layer, for Mg_yNi films with $1.7 < y < 2$ the predominant effect is the growth of the transparent Mg_2NiH_4 layer formed at the substrate interface. A direct determination of the internal structure of $\text{Mg}_{2\pm\delta}\text{Ni}$ films during hydrogenation is not straightforward since these films are X-ray amorphous. We show however that valuable information can be deduced from a combination of optical reflection and transmission spectra measured simultaneously together with

* Corresponding author.

E-mail address: dborsa@few.vu.nl (D.M. Borsa).

electrical resistivity during exposure of thin $\text{Mg}_{2\pm\delta}\text{Ni}$ films to hydrogen.

2. Experimental details

Mg_xNi thin films of various composition are prepared by dc magnetron co-sputtering at room temperature from a Mg and a Ni target on sapphire substrates in a vacuum chamber (base pressure $\sim 10^{-6}$ Pa). Two composition regions are studied: (a) slightly sub-stoichiometric Mg_2Ni films ($1.7 < x < 2$) and (b) slightly over-stoichiometric Mg_2Ni films ($2 < x < 2.5$). The films are 200 nm thick and have a 10 nm Pd layer on top. A Pd layer is needed to promote dissociation of H_2 and to prevent oxidation of the underlying film. The results discussed in this article are measured on $\text{Mg}_{1.85}\text{Ni}$ and $\text{Mg}_{2.05}\text{Ni}$. These results are representative for samples in the composition ranges mentioned above. This choice of compositions is dictated by the room temperature phase diagram of Mg–Ni binary alloys which contains only two intermetallic compounds: Mg_2Ni and MgNi_2 [10]. An amorphous phase with $\text{Mg}:\text{Ni}=1$ was also reported to be present in mechanically alloyed powder samples [11]. Based on these data, $\text{Mg}_{2.05}\text{Ni}$ corresponds to almost stoichiometric Mg_2Ni (possibly with some extra Mg) whereas $\text{Mg}_{1.85}\text{Ni}$ is a mixture of Mg_2Ni and a small amount of pure MgNi_2 or the MgNi phase. For bulk Mg–Ni samples [11], it is often reported that due to incomplete reaction of the metals, phases such as Ni and/or MgNi_2 are also present both in slightly over- and under-stoichiometric Mg_2Ni alloys. We do not have any indications that incomplete reaction between the co-sputtered metals occurs in our thin films. However, the presence of small quantities of additional phases such as MgNi_2 and Ni cannot be excluded. The Mg_2Ni phase reacts with hydrogen to form the Mg_2NiH_4 phase. According to Reilly and Wiswall [12], the MgNi_2 phase does not react with hydrogen in the crystalline phase. On the other hand, Orimo and Fujii [11] reported that mechanical grinding does promote a hydriding reaction of MgNi_2 to form a $\text{MgNi}_2\text{H}_{0.7}$ phase even at room temperature. Moreover, they reported that the amorphous-like MgNi phase also reacts with hydrogen to form a $\text{MgNiH}_{1.9}$ phase. From all these hydrides, only the Mg_2NiH_4 phase is known to be transparent. The composition and the thickness of the films are checked ex situ by Rutherford Backscattering spectrometry measurements on films grown in the same deposition run but on carbon substrates. No compositional gradient within a film is found. Optical measurements are performed in a Bruker IFS66 Fourier transform spectrometer (0.72–3.5 eV) that measures simultaneously reflection and transmission during hydrogenation (pressures up to 1 bar H_2). The reflection and the transmission are measured at near normal incidence of the incoming beam. To reduce the influence of the Pd cap layer and surface roughness, all the optical measurements are done through the transparent substrate. The resistivity of the films is measured simultaneously with the optical properties in a four-point Van der Pauw configuration [9].

3. Results

3.1. Experimental data

Fig. 1 shows the reflection, transmission (both at $\hbar\omega = 1.65$ eV) and electrical resistivity upon hydrogenation at room temperature measured at a constant pressure of 20 mbar H_2 . The optical reflection features a dramatic drop in the early stage of the hydrogenation process for both compositions. The transmission is practically zero and the electrical resistivity has still metallic character. This corresponds to the so-called black state, which

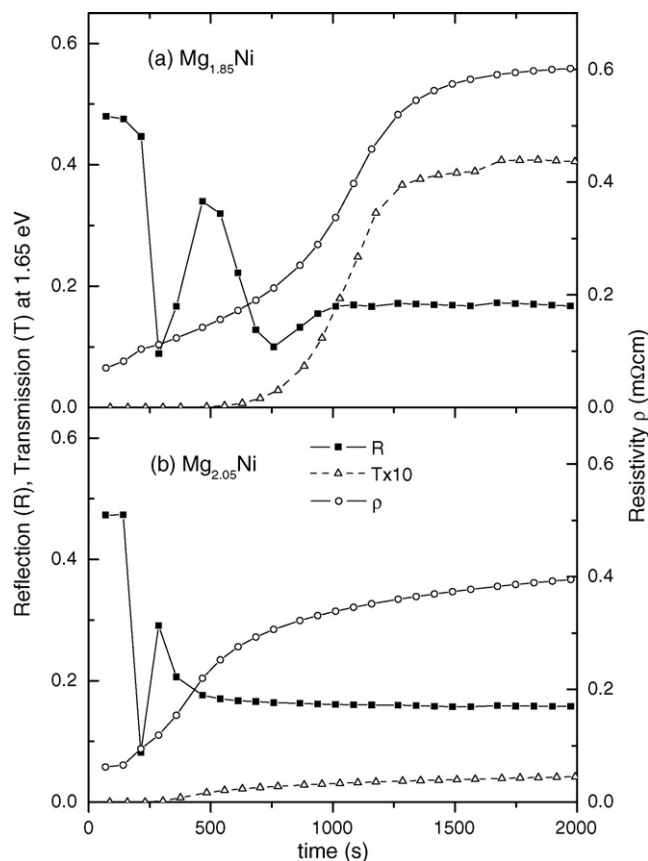


Fig. 1. Optical reflection and transmission at $\hbar\omega = 1.65$ eV measured simultaneously with the electrical resistivity during hydrogenation: (a) $\text{Mg}_{1.85}\text{Ni}$ and (b) $\text{Mg}_{2.05}\text{Ni}$. The films are 200 nm thick and are capped with 10 nm Pd. The hydrogen pressure is 20 mbar H_2 . The temperature is 293 K. For reasons of clarity the optical transmission is multiplied by a factor 10.

is observed for a large part of the solar spectrum ($0.5 < \hbar\omega < 4$ eV). A major difference between the two types of samples is observed on further hydrogenation. For the sub-stoichiometric film (Fig. 1(a)), the reflection has an oscillating behavior while the resistivity follows a steep increase. This is followed by a region of rather constant reflection and a slowly increasing resistivity. For the slightly over-stoichiometric film (Fig. 1(b)) the reflection decreases only slightly while the resistivity increases. The optical transmission of $\text{Mg}_{1.85}\text{Ni}$ reached after 2000 s (in 20 mbar H_2) is a factor ten higher than the one corresponding to $\text{Mg}_{2.05}\text{Ni}$. This suggests that in this case more transparent hydride phase is formed than in the sub-stoichiometric film. In contrast, the difference between the resistivity of the two films is much less pointing to a different internal structure. For the over-stoichiometric film, the combination of low transmission and rather high resistivity indicates a preferential nucleation and growth of the transparent hydride maybe along grain boundaries. Another possibility could be that the hydride phase starts to form at the surface of the crystallites. Such a surface layer could act as a barrier for further hydride formation. The low transmission of the films after 2000 s may also indicate that these samples did not reach yet the fully hydrogenated state. A further increase in the transmission and the electrical resistivity can indeed be obtained by applying higher hydrogen pressures. In the final

hydrogenated state, both films have similar electrical resistivity that is close to $0.75 \text{ m}\Omega \text{ cm}$ (not corrected for the Pd layer). On the other hand, the optical transmission of $\text{Mg}_{1.85}\text{Ni}$ ($\sim 6\%$ at 1.65 eV) is significantly higher than that of $\text{Mg}_{2.05}\text{Ni}$ ($\sim 3\%$ at 1.65 eV). For both compositions, the predominant phase is Mg_2Ni that transform to transparent Mg_2NiH_4 upon hydrogen absorption. In sub-stoichiometric films, the secondary phase does not absorb hydrogen. Consequently, in a fully hydrogenated state situation, one would expect a lower transmission for $\text{Mg}_{1.85}\text{Ni}$ as compared to $\text{Mg}_{2.05}\text{Ni}$. This is not the case here indicating an inhomogeneity in the internal structure of the partly hydrogenated films that prevents complete hydrogenation of the metal phase.

3.2. Calculated data

It is quite surprising that a small change in composition can induce such large differences in optical properties and therefore, in the hydrogen uptake mechanism and the amount of hydride formed. As described in Section 3.1, the observed differences point to a different nucleation and growth process of the hydride. To verify the validity of our intuitive interpretation we compare the measured data to calculations for specific sample configurations. More specifically we calculate the optical response and the electrical resistivity corresponding to three systems: (i) a double layered structure of $\text{Mg}_2\text{NiH}_{0.3}$ and Mg_2NiH_4 (at the substrate interface); upon loading the Mg_2NiH_4 layer grows in thickness at the expense of the $\text{Mg}_2\text{NiH}_{0.3}$ layer until the entire

film has switched; (ii) a single composite layer of $\text{Mg}_2\text{NiH}_{0.3}$ and Mg_2NiH_4 ; (iii) a layer of Mg_2NiH_4 (at the substrate interface) of fixed thickness (60 nm) and a composite top layer consisting of $\text{Mg}_2\text{NiH}_{0.3}$ and Mg_2NiH_4 . A schematic drawing of the three geometries is given in Fig. 2(a)–(c). The optical properties of a mixture of two materials A and B can be modelled using the Bruggeman effective medium approximation [13] if the particle sizes are smaller than the wavelength of light. This model however does not discriminate between more inclusions and larger inclusions. According to X-ray diffraction measurements [7], our films are either nanocrystalline (with nanosized crystallites) or amorphous. Consequently, the Bruggeman effective medium approximation can be applied. In this model,

$$f_A \frac{\epsilon_A - \langle \epsilon \rangle}{L\epsilon_A + (1-L)\langle \epsilon \rangle} + f_B \frac{\epsilon_B - \langle \epsilon \rangle}{L\epsilon_B + (1-L)\langle \epsilon \rangle} = 0 \quad (1)$$

where $\langle \epsilon \rangle$, ϵ_A and ϵ_B are the complex dielectric functions of the effective medium ($\epsilon(\omega) = \epsilon_1(\omega) + i\epsilon_2(\omega)$) consisting of phase A ($\text{Mg}_2\text{NiH}_{0.3}$) and phase B (Mg_2NiH_4); f_A and f_B are the corresponding volume fractions ($f_A + f_B = 1$); L is a geometric factor that depends on the shape of the inclusions ($0 \leq L \leq 1$). Here we assume spherical inclusions ($L = \frac{1}{3}$). The transfer matrix method [14] is used to calculate the reflection and transmission of the total sample also taking into account the sapphire substrate and the Pd cap layer [15]. For the switching $\text{Mg}_{2\pm\delta}\text{Ni}$ layer, the dielectric function of the single phases Mg_2Ni , $\text{Mg}_2\text{NiH}_{0.3}$, Mg_2NiH_4 [7] and the effective dielectric function derived from

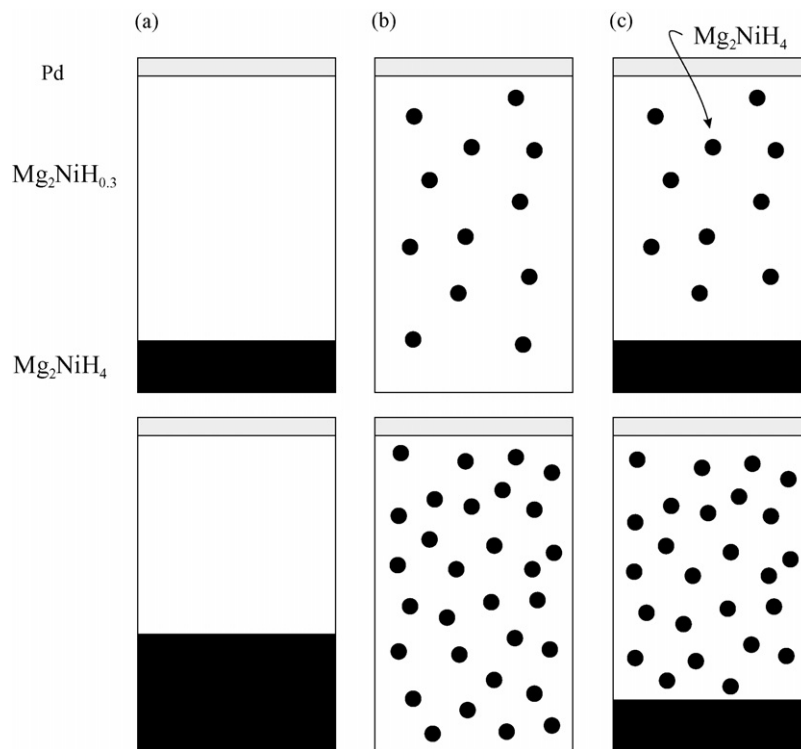


Fig. 2. Schematic drawing of three possible hydrogenation scenarios. In the top panels: (a) double layer structure of Mg_2NiH_4 and $\text{Mg}_2\text{NiH}_{0.3}$; (b) mixed layer of $\text{Mg}_2\text{NiH}_{0.3}$ and Mg_2NiH_4 ; (c) double layer of Mg_2NiH_4 and a mixed layer of $\text{Mg}_2\text{NiH}_{0.3}$ and Mg_2NiH_4 . A step further in the hydrogenation process is shown in the lower panels.

the Bruggeman approximation (for the $\text{Mg}_2\text{NiH}_{0.3}$ – Mg_2NiH_4 composite) are used. The only parameter varied in the calculations is the volume fraction f_B of Mg_2NiH_4 . A zero fraction corresponds to a pure $\text{Mg}_2\text{NiH}_{0.3}$ layer. For comparison with the experimental data we also calculate the reflection and the transmission of Mg_2Ni . These data are plotted also at $f_B = 0$. For modelling the electrical properties of a mixture of two materials A and B we can apply again the Bruggeman effective medium approximation [13]. The effective electrical resistivity (ρ) of a $\text{Mg}_2\text{NiH}_{0.3}$ – Mg_2NiH_4 composite is obtained from the electrical resistivity of the single phases: $\text{Mg}_2\text{NiH}_{0.3}$ ($\rho_A = 80 \mu\Omega\text{cm}$) and Mg_2NiH_4 ($\rho_B = 12.96 \text{m}\Omega\text{cm}$ [16]) using

$$f_A \frac{\rho_A - \rho}{L\rho + (1-L)\rho_A} + f_B \frac{\rho_B - \rho}{L\rho + (1-L)\rho_B} = 0 \quad (2)$$

with f_A and f_B the corresponding volume fractions ($f_A + f_B = 1$) and L the geometric factor ($L = \frac{1}{3}$ for spherical inclusions). To simulate the experiments, we assume a double layer model with 10 nm Pd ($\rho = 75 \mu\Omega\text{cm}$) in parallel with the 200 nm $\text{Mg}_2\text{NiH}_{0.3}$ – Mg_2NiH_4 layer. Also here we take $f_B = 0$ to correspond to $\text{Mg}_2\text{NiH}_{0.3}$. The electrical resistivity of Mg_2Ni ($\rho = 60 \mu\Omega\text{cm}$) with a 10 nm Pd on top is calculated and plotted at $f_B = 0$. A complete transformation of Mg_2Ni into Mg_2NiH_4 is accompanied by a 32% volume expansion. In our calculations, the variation in thickness given by the hydride formation is also included (both for the optical properties and the electrical resistivity). For the sake of simplicity, we assume a completely hydrogenated bottom hydride layer. The results are shown in Fig. 3. The resemblance between Figs. 3(c) and 1(b) suggests that in $\text{Mg}_{2.05}\text{Ni}$, after the initial double layer formation, the growth of the Mg_2NiH_4 layer at the substrate–film interface stops. The hydrogenation process appears to proceed further by random nucleation of Mg_2NiH_4 in the upper layer. This second process is quite slow. For $\text{Mg}_{1.85}\text{Ni}$, the experimental data are much better reproduced by the model schematically shown in Fig. 2(a) corresponding to the further growth of the bottom Mg_2NiH_4 layer. However, the convex shape of the resistance curve observed after $t = 1200$ s and the constant reflection suggest a competition with a random nucleation process in the last stages of the hydrogenation process.

3.3. Discussion

The dramatic drop in reflection observed in the initial stages of the hydrogenation process was argued to be typical for Mg_2NiH_x films and to be the result of a self-organized double layering caused by a preferential nucleation of Mg_2NiH_4 at the film–substrate interface [2,7] and not as intuitively expected, close to the catalytic Pd layer at the surface. The reflection minimum and the zero transmission was originally reproduced by assuming a 30 nm thick nucleating layer consisting of 20% $\text{Mg}_2\text{NiH}_{0.3}$ and 80% Mg_2NiH_4 in the vicinity of the substrate and a top $\text{Mg}_2\text{NiH}_{0.3}$ layer [2,7]. This $\text{Mg}_2\text{NiH}_{0.3}$ phase corresponds to the solid solution phase and is formed first upon hydrogenation of Mg_2Ni . An enhanced concentration of hydrogen at the film–substrate interface corresponding to a hydrogenated Mg_2NiH_x layer was confirmed by ^{15}N hydrogen depth profiling

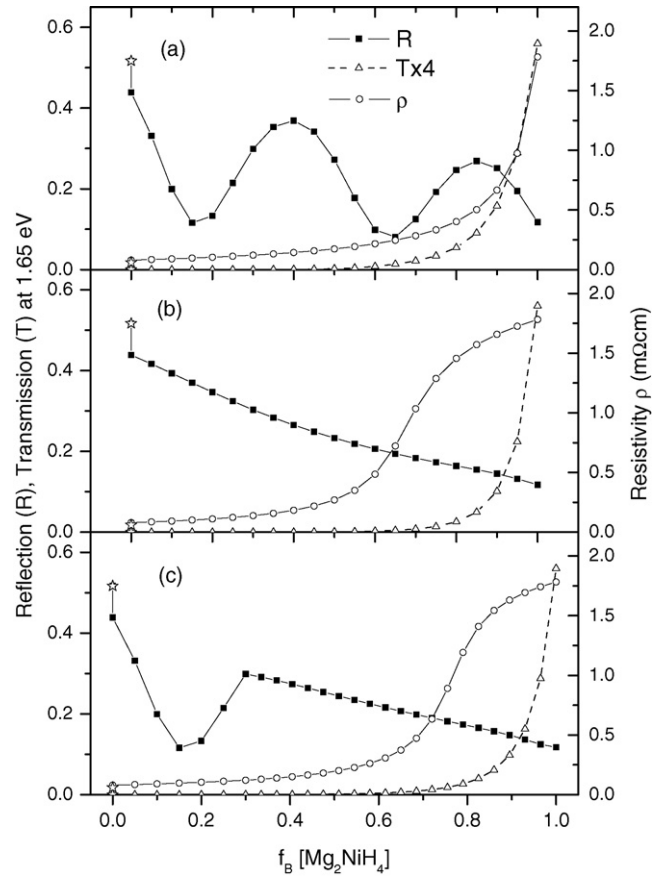


Fig. 3. Calculated reflection, transmission (both at $\hbar\omega = 1.65$ eV) and resistivity of a 200 nm thick $\text{Mg}_2\text{NiH}_{0.3}$ – Mg_2NiH_4 film covered with 10 nm Pd as a function of the volume fraction of Mg_2NiH_4 (f_B). The geometries considered are shown in Fig. 2(a)–(c) as follows: (a) double layer structure of Mg_2NiH_4 and $\text{Mg}_2\text{NiH}_{0.3}$; (b) mixed layer of $\text{Mg}_2\text{NiH}_{0.3}$ and Mg_2NiH_4 ; (c) a 60 nm Mg_2NiH_4 nucleating layer at the film–substrate interface and a mixed layer of $\text{Mg}_2\text{NiH}_{0.3}$ and Mg_2NiH_4 on top. The reflection, transmission and resistivity of Mg_2Ni is calculated and plotted also at $f_B = 0$ (\star). For reasons of clarity transmission is multiplied by a factor 4.

measurements [7]. As concluded from extensive microstructural investigations on Mg_2Ni thin films [8], at the substrate–film interface, the films have a peculiar local microstructure, which is different from the rest of the films. By combining results from TEM cross-section, STM/AFM and SEM micrographs, Westerwaal et al. [8] showed that the films consist of a high density of loosely packed nanograins only at the interface with the substrate whereas in the rest of the films, columns separated by grain boundary channels were identified. It is therefore likely that the part of the film near the substrate interface (typical 30–50 nm) is more favorable for hydrogenation than the rest of the film (typical 150–170 nm), e.g., the enthalpy is more negative in the region closer to the substrate than in the rest of the film. The depth dependence of the microstructure of Mg–Ni films leads to a peculiar time dependence of the hydrogen concentration in the films. To illustrate this point we consider the following idealized situation. We model our films as a double layer system made of layer C (with columnar grains) and N (with nanograins). The enthalpy of hydride formation ΔH_N is assumed to be more

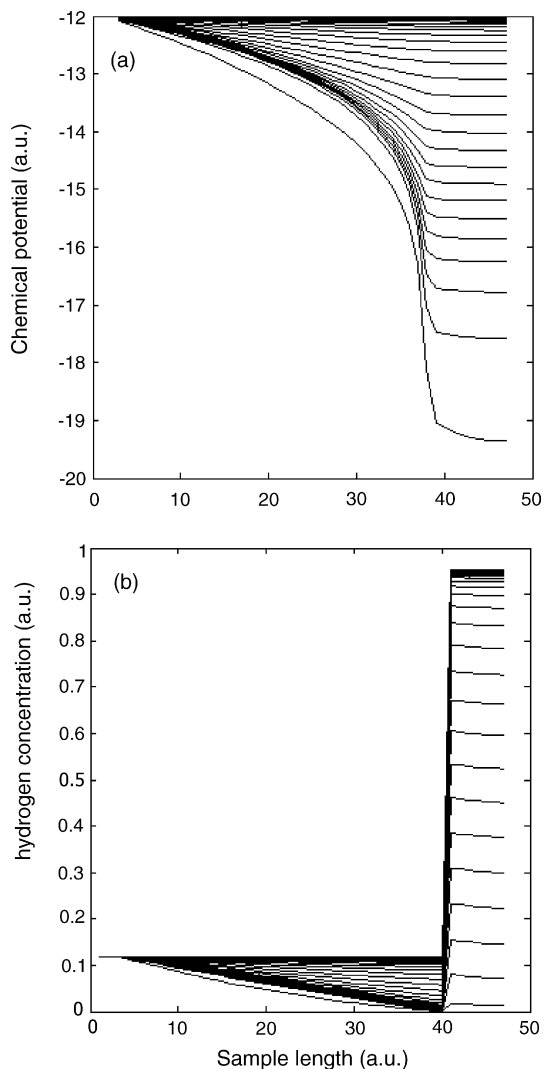


Fig. 4. (a) Profiles of the chemical potential of hydrogen in time and sample depth. (b) Concentration profile in the sample. Clearly visible is the high concentration in the thin layer near the ‘substrate’ on the right. The lowest profile corresponds to $t = 1$ time step; the top one to 12 time steps.

negative than ΔH_C , the enthalpy of hydride formation in the columnar region. The evolution in time of the chemical potential and the hydrogen concentration profiles in this double layer system is obtained by solving numerically the diffusion equation considering that: (i) at equilibrium the chemical potential is the same everywhere, (ii) the current of hydrogen in a material is proportional to the gradient of the chemical potential μ_H of hydrogen, i.e. $J_H = -L\nabla\mu_H$ [17]. In Fig. 4 we show results obtained for a two-layer model (50 units thick). For the N-layer (10 units thick) we have chosen $\Delta H/kT = -15$ ($\Delta H =$ enthalpy) and for the C-layer $\Delta H/kT = -10$. The chemical potential of H_2 gas is chosen as $\mu/kT = -12$; The parameter L is related to the diffusion coefficient D through the relation $L = Dcc_0/kT$ (c : concentration, c_0 : maxim concentration in the system); the diffusion coefficient is chosen as $5 \times 10^{-6} \text{ cm}^2/\text{s}$. As shown here, in a system where hydrogen diffuses from the C-layer (i.e. from the Pd side in the real sample) to the N-layer (i.e.

to the substrate side), the chemical potential in the C-layer decreases steadily from the Pd side to the substrate side (Fig. 4(a)) whereas the concentration of hydrogen in the N-layer (i.e. near the substrate) is clearly larger than in the rest of the film (Fig. 4(b)). This example shows clearly that is very well possible to have a higher concentration near the substrate than in the rest of the sample provided an inhomogeneity in thermodynamic properties.

Beyond the first stage of nucleation and growth at the substrate interface, Lohstroh et al. [7] proposed the following hydrogenation sequence: first the nucleating layer loads completely to Mg_2NiH_4 and subsequently grows in thickness until the whole film has switched. No correlation between the loading behavior and composition was reported [7]. However, as shown here, we do find a strong correlation between composition and the hydrogenation sequence following the appearance of the black state. It appears that there is a competition between random nucleation of Mg_2NiH_4 within the upper $Mg_2NiH_{0.3}$ layer and the growth of the initial Mg_2NiH_4 layer at the expense of the upper metallic part. In under-stoichiometric films, the H-loading is *fast* and proceeds mainly through the growth of the initial Mg_2NiH_4 layer. In over-stoichiometric films the hydrogen loading becomes *slow* after the nucleation of the initial interface layer. It appears as if the growth of this layer is blocked. The hydrogenation process now mainly proceeds through random nucleation within the upper metal layer. As the transmission remains low on further loading, we conclude that also the growth of these secondary nuclei is hindered. The reason for this is not directly obvious. According to Zeng [18], in over-stoichiometric Mg_2Ni alloys first MgH_2 is formed while the remaining (stoichiometric) alloy transforms into Mg_2NiH_4 only on further hydrogenation. It is hard to imagine why small amounts of MgH_2 phase would have such a large effect on the growth of the Mg_2NiH_4 phase, unless when they act as blocking impurities [19]. In that case, the growth of the initial hydride layer would be blocked, favoring the formation of secondary nuclei. In turn, these secondary nuclei may also get blocked by impurities which would explain the low transmission we obtain in this case. The fact that we nevertheless observe a high resistivity (Fig. 1(b)), indicates some ordering of the secondary nuclei, e.g., at the columnar grain boundaries.

Recently, the stability and the optical properties of Mg_2NiH_4 was linked to the microtwinning observed in bulk samples of this material. Changes in the twinning structure could be induced by mechanical pressure [20] and oxygen contamination [21]. These optical changes involve a change in color and therefore most probably in bandgap. Our films have a very low oxygen impurity level. This would therefore not influence the optical and electrical properties. The microtwinning observed in the Mg_2NiH_4 bulk alloys, is, however, not very likely to be present in our films. Here, the Mg_2NiH_4 phase forms at room temperature during hydrogenation at moderate pressures (up to 1 bar H_2). It is not subjected to the high-to-low temperature phase transition at which the microtwinning is formed. The microstructure is either nanocrystalline or amorphous, with a grain size less than 30 nm. We have no evidence that microtwinning actually occurs in our films. The optical effects we observe can

be understood by a different arrangement of the same materials involved.

The present results also illustrate that the over-stoichiometric films have a very high optical absorption almost for the entire hydrogenation period as a result of the particular nucleation and growth. Whereas the initial black state is a result of a self-organized double layering, the mechanism giving rise to the extended black state is similar to the black state observed in the Mg–MgH₂ composite [22] at intermediate hydrogen concentrations. In this case, it was shown that the key ingredient is the coexistence of metallic and semiconducting nanograins that are homogeneously dispersed over the entire film thickness.

4. Conclusion

We have shown that by combining optical and electrical measurements with calculations of the expected reflection, transmission and electrical resistivity using a transfer matrix method and a mean-field model (Bruggeman) we can obtain valuable information on the internal structure of Mg_{2±δ}Ni films during hydrogenation. We find that after the initial formation of a thin Mg₂NiH₄ layer at the substrate-film interface, the ensuing hydrogenation process is characterized by a competition between the growth of the initial Mg₂NiH₄ layer (fast) and the random nucleation (slow) of the same phase but within the upper metallic layer. Which process dominates depends critically on the stoichiometry of the metal alloy and determines the evolution of the optical and electrical properties. If these materials were to be used as switchable mirrors one can tune their optical response by varying the composition and opt either for a homogeneous absorbing state (Mg-rich) or a variable reflectance state (Mg-poor). For the application as hydrogen storage materials our results highlight and underline the importance of phase nucleation in the transformation kinetics in these complex metal hydrides. Our results show that during hydrogenation the hydride does not necessarily form at the surface of the metal, but may also nucleate within the bulk of the material.

Acknowledgment

This work is part of the research program of the Stichting Technologische Wetenschappen (STW) and Stichting voor Fundamenteel Onderzoek der Materie (FOM).

References

- [1] J. Isidorsson, I.A.M.E. Giebels, R. Griessen, M.Di. Vece, *Appl. Phys. Lett.* 80 (2002) 2305.
- [2] W. Lohstroh, R.J. Westerwaal, B. Noheda, S. Enache, I.A.M.E. Giebels, B. Dam, R. Griessen, *Phys. Rev. Lett.* 93 (2004) 197404.
- [3] J.L.M. van Mechelen, B. Noheda, W. Lohstroh, R.J. Westerwaal, J.H. Recor, B. Dam, R. Griessen, *Appl. Phys. Lett.* 84 (2004) 3651.
- [4] R. Armitage, M. Rubin, T. Richardson, N. O'Brien, Y. Chen, *Appl. Phys. Lett.* 75 (1999) 1863.
- [5] V.M.M. Mercier, P. Sluis Van der, *Solid State Ionics* 145 (2001) 17.
- [6] D. Lupu, R. Sarbu, A. Biris, *Int. J. Hydrogen Energy* 12 (1987) 1987.
- [7] W. Lohstroh, R.J. Westerwaal, J.L.M. van Mechelen, C. Chacon, E. Johansson, B. Dam, R. Griessen, *Phys. Rev. B* 70 (2004) 165411.
- [8] R.J. Westerwaal, A. Borgschulte, W. Lohstroh, B. Kooi, G. ten Brink, M.J.P. Hopstaken, P.H.L. Notten, B. Dam, *J. Alloys Compd.* 416 (2006) 2–10.
- [9] L.J. van der Pauw, *Phillips Res. Repts.* 13 (1958) 1.
- [10] A.A. Neyeb-Hashemi, J.B. Clark, *Phase Diagrams of Binary Magnesium Alloys*, vol. 4 of Monograph series on Alloy Phase Diagrams (ASM International, Ohio, 1988).
- [11] S. Orimo, H. Fujii, *Appl. Phys. A* 72 (2001) 167.
- [12] J.J. Reilly, R.H. Wiswall Jr., *Inorg. Vehm.* 7 (1968) 2254.
- [13] D.A.G. Bruggeman, *Ann. Phys. (Leipzig)* 24 (1935) 636.
- [14] M. Born, E. Wolf, *Principles of Optics*, University Press, Cambridge, 1980.
- [15] E.D. Palik (Ed.), *Handbook of Optical Constants of Solids*, vols. I–III, Academic Press, San Diego, 1998.
- [16] S. Enache, W. Lohstroh, R. Griessen, *Phys. Rev. B.* 69 (2004) 115326.
- [17] P.G. Shewmon, *Diffusion in solids*, McGraw-Hill Book Company Inc., New York, 1963.
- [18] K. Zeng, T. Klassen, W. Oelerich, R. Bormann, *J. Alloys Comp.* 283 (1999) 213.
- [19] W.J.P. van Enckevort, A.C.J.F. van den Berg, *J. Crystal Growth* 183 (1998) 441.
- [20] H. Blomqvist, D. Noréus, *J. Appl. Phys.* 91 (2002) 5141.
- [21] E. Rönnebro, D. Noréus, *Appl. Surf. Sci.* 228 (2004) 115.
- [22] I.A.M.E. Giebels, J. Isidorsson, R. Griessen, *Phys. Rev. B* 69 (2004) 205111.